

## A Bifunctional 2D Cd(II)-Based Metal-Organic Framework as Efficient Heterogeneous Catalyst for the Formation of C-C Bond

Lei Hu, Gui-Xia Hao, Hai-Dong Luo, Chun-Xian Ke, Guang Shi,  
Jia Lin, Xiao-Ming Lin, Umair Yaqub Qazi, and Yue-Peng Cai

*Cryst. Growth Des.*, **Just Accepted Manuscript** • Publication Date (Web): 26 Mar 2018

Downloaded from <http://pubs.acs.org> on March 26, 2018

### Just Accepted

“Just Accepted” manuscripts have been peer-reviewed and accepted for publication. They are posted online prior to technical editing, formatting for publication and author proofing. The American Chemical Society provides “Just Accepted” as a service to the research community to expedite the dissemination of scientific material as soon as possible after acceptance. “Just Accepted” manuscripts appear in full in PDF format accompanied by an HTML abstract. “Just Accepted” manuscripts have been fully peer reviewed, but should not be considered the official version of record. They are citable by the Digital Object Identifier (DOI®). “Just Accepted” is an optional service offered to authors. Therefore, the “Just Accepted” Web site may not include all articles that will be published in the journal. After a manuscript is technically edited and formatted, it will be removed from the “Just Accepted” Web site and published as an ASAP article. Note that technical editing may introduce minor changes to the manuscript text and/or graphics which could affect content, and all legal disclaimers and ethical guidelines that apply to the journal pertain. ACS cannot be held responsible for errors or consequences arising from the use of information contained in these “Just Accepted” manuscripts.



# A Bifunctional 2D Cd(II)-Based Metal-Organic Framework as Efficient Heterogeneous Catalyst for the Formation of C-C Bond

Lei Hu,<sup>†</sup> Gui-Xia Hao,<sup>‡</sup> Hai-Dong Luo,<sup>†</sup> Chun-Xian Ke,<sup>†</sup> Guang Shi,<sup>†</sup> Jia Lin,<sup>†</sup> Xiao-Ming Lin,<sup>\*,†, §</sup> Umair Yaqub Qazi,<sup>||</sup> and Yue-Peng Cai<sup>\*,†</sup>

<sup>†</sup>*School of Chemistry and Environment, South China Normal University, Guangzhou Key Laboratory of Materials for Energy Conversion and Storage, 510006, P.R. China*

<sup>‡</sup>*College of Chemistry and Environmental Engineering, Hanshan Normal University, Chaozhou, Guangdong, 521041, P.R. China*

<sup>§</sup>*State Key Laboratory of Structural Chemistry, Fujian Institute of Research on the Structure of Matter, Chinese Academy of Sciences, Fuzhou, Fujian, 350002, P.R. China*

<sup>||</sup>*Division of Nanomaterials and Chemistry, Hefei National Laboratory for Physical Sciences at Microscale, University of Science and Technology of China, Hefei, 230026, China*

**ABSTRACT:** A porous two-dimensional (2D) metal-organic framework (MOF), namely, [Cd(PBA)(DMF)] DMF (Cd-PBA), has been solvothermally synthesized by the reaction of 5-(4-pyridin-3-yl-benzoylamino)-isophthalic acid ligand (H<sub>2</sub>PBA) and Cd(II) ions. Structural analysis shows that Cd-PBA possesses 2D (3,6)-connected kgd net topology with the Schläfli symbol of (4<sup>3</sup>)<sub>2</sub>(4<sup>6</sup>.6<sup>6</sup>.8<sup>3</sup>) and exhibits two distinct types of 1D opening channels along *a*- and *c*-axis. The incorporation of Cd metal centers and -NH groups of amides endows Cd-PBA rich open metal sites and Lewis basic sites, which are applied as an efficient catalyst for the important Knoevenagel condensation and cyanosilylation of aldehydes reactions. This Cd-PBA presents highly efficient catalytic activity and recyclability for both Knoevenagel condensation reaction and cyanosilylation of various aldehydes with trimethylsilyl cyanide (TMSCN). The excellent catalytic activity can be maintained at least four cycles without loss of obvious catalytic activity. These results indicate Cd-PBA can serve as a promising heterogeneous catalyst toward C-C bond formation due to the stability and high catalytic activity.

## 1. INTRODUCTION

Nowadays, porous metal-organic frameworks (MOFs), as the particular field of materials science, is being extensively studied due to their intriguing topologies and the multifunctional properties, such as separation and gas storage, catalysis science, magnetism, luminescence, *etc.*<sup>1-9</sup>. Particularly interesting are those related to the application of heterogeneous catalysis. It is feasible and fundamental to predict the possible catalytic properties and activity through reasonable design and fine characterization of these materials.<sup>10-14</sup> For instance, the selection of ligand and metal center can direct the structural diversity with variable topological structures, and accessibility to the active center.<sup>15</sup> Generally speaking, one effective strategy is to create coordinatively unsaturated metal sites or introduce nanosized metallic clusters/organometallic complexes into the MOFs through post-modification method.<sup>16-19</sup> Another effective strategy is to fabricate functionalized ligands to synthesize desired MOFs.<sup>20,21</sup>

We have been studying on the design of functionalized MOFs and application for heterogeneous catalysis.<sup>22-24</sup> As reported in our previous work, we obtained a polyhedral

metal-organic framework, [Eu<sub>2</sub>(PDC)<sub>3</sub>] (H<sub>2</sub>PDC=pyridine-3,5-dicarboxylic acid), which could effectively accelerate the cyanosilylation reaction.<sup>25</sup> By utilizing of a versatile Cu<sup>II</sup>/Cu<sup>I</sup> metal-organic framework as catalyst, three-component coupling reactions of diisopropylamine, tosylazide, and aromatic alkynes can be promoted as well as the oxidation of benzylic compounds.<sup>26</sup> As part of our continuous work, herein, we reported the synthesis and characterization of a 2D (3,6)-connected framework with kgd topology, namely, [Cd(PBA)(DMF)] DMF, (H<sub>2</sub>PBA=5-(4-pyridin-3-yl-benzoylamino)-isophthalic acid). Moreover, the catalytic properties were also studied.

## 2. EXPERIMENTAL SECTION

**2.1. General Information.** Organic ligand was synthesized based on the procedures described previously.<sup>27-29</sup> All reagents and solvents employed were purchased from commercial sources and used without further purification. Infrared spectra were collected from KBr pellets on a Nicolet/Nexus-670 FT-IR spectrometer. Perkin-Elmer 240 elemental analyzer was used to carry out the elemental analyses. Thermogravimetric analyses (TGA) were performed on a Netzsch Thermo Microbalance TG 209 F3 Tarsus from room temperature to

900 °C under flowing nitrogen. X-ray powder diffraction patterns were characterized on a Bruker D8 Advance diffractometer with Cu target tube. A Varian 500 MHz spectrometer was used to record <sup>1</sup>H NMR spectra. Quantachrome Autosorb-iQ-MP gas sorption analyzer was applied to measure sorption isotherms. The size and shape were characterized by using field emission scanning electron microscopy (FESEM, TESCAN Maia 3, Czech) operating at 5 kV and transmission electron microscopy (TEM, JEM-2100HR, Japan) coupled with an acceleration voltage of 200 kV.

**2.2 Preparation of [Cd(PBA)(DMF)] DMF.** A mixture containing H<sub>2</sub>PBA (72.4 mg, 0.2 mmol), Cd(NO<sub>3</sub>)<sub>2</sub> · 4H<sub>2</sub>O (60 mg, 0.2 mmol), and dimethylformamide (DMF, 6 mL) was sealed in a glass reaction bottle. The system was heated at 90 °C for 3 d and then cooled to room temperature. Block crystals were obtained by filtration and washed with DMF. FT-IR (KBr, cm<sup>-1</sup>): 3366 (s), 1646 (vs), 1558 (w), 1425 (w), 1394 (w), 1307 (w), 782 (w), 717 (w). Anal. calcd for C<sub>26</sub>H<sub>26</sub>N<sub>4</sub>O<sub>7</sub>Cd (618.91): C 50.46, H 4.23, N 9.05 %; found: C 50.42, H 4.27, N 9.03 %.

**2.3. X-Ray Structure Determination.** X-ray reflection intensities were performed with a Bruker APEX II diffractometer at 296 K using graphite monochromatic Mo-K $\alpha$  radiation ( $\lambda=0.71073$  Å). The empirical absorption corrections were used to correct the reflections. The structure was solved by the direct method and refined by full-matrix least-squares on  $F^2$  using SHELXL programs (SHELXTL-2014).<sup>30</sup> The non-hydrogen atoms were refined with anisotropic displacement parameters at the final cycles. Isotropic displacement parameter was used to place the organic hydrogen atoms in calculated positions. The details of the crystal parameters, data collection, and refinement are summarized in Table S1, and the selected bond lengths are listed in Table S2. CCDC 1580065 contains the crystallographic data.

**2.4. Sample Activation.** Prior to the catalytic test, the as-prepared Cd-PBA samples were soaked in CH<sub>3</sub>OH for three days. Further, the samples were filtrated and dried at 120 °C for 5 h under vacuum to remove the physical and chemical guest molecules, generating the dehydrated phase Cd-PBA.

**2.5. Typical Procedure for Knoevenagel condensation reaction.** In a 10 mL Pyrex-glass screw-cap vial were placed successively benzaldehyde (100  $\mu$ L, 1 mmol), malononitrile (111  $\mu$ L, 2 mmol), ethanol (5 mL), and activated Cd-PBA (9.5 mg, 0.02 mmol, 2 %). Then the mixture was stirred with a Teflon-coated magnetic stir at room temperature for 2 h. After that, the supernatant was filtered and concentrated under reduced pressure. The reaction crudes were further purified by flash column chromatography and the yields of the reaction products were determined by <sup>1</sup>H NMR spectroscopy by using dibromomethane as an internal standard.

**2.6. Typical Procedure for Cyanosilylation Reaction.** A mixture of benzaldehyde (26.5 mg, 0.25 mmol), trimethylsilyl cyanide (TMSCN, 49.6 mg, 0.5 mmol), and *n*-hexane (5 mL) was placed into a Pyrex-glass screw-cap vial (10 mL), and Cd-PBA catalyst (2 %) was added and the resulting reaction mixture was stirred with a Teflon-coated magnetic stir at room temperature for 8 h. The yields were determined by <sup>1</sup>H NMR analysis using dibromomethane as an internal standard.

### 3. RESULTS AND DISCUSSION

#### 3.1. Structure and Characterization of Cd-PBA MOF.

Structural analysis reveals that Cd-PBA crystallizes in the triclinic  $P\bar{1}$  space group. As depicted in Figure 1a, the Cd ion is six-coordinated and exhibits an octahedral coordination surrounded by one N atom, four carboxylate oxygen atoms of three different PBA<sup>2-</sup> ligands, and one oxygen atom from a coordinated DMF molecule. The neighboring Cd(II) ions are connected together through the carboxylate groups of PBA<sup>2-</sup> ligands to form a 1D infinite chain (Figure 1b), in which the carboxylate groups adopt the bidentate chelating and bidentate bridging coordination modes. These chains are further linked by PBA<sup>2-</sup> ligands using the N atoms to give rise to a 2D layer network (Figure 1c). A better insight into the nature of this structure can be achieved by the application of a topology approach, each PBA<sup>2-</sup> ligand acts as organic trinodal building block and the binuclear cadmium atoms serve as hexatopic node geometry (Figure S1). Thus, the whole framework can be ascribed as a binodal (3,6)-connected kagomé dual (**kgd**) net topology with the Schläfli symbol of  $(4^3)_2(4^6.6^6.8^3)$  analyzed by *Topos 4.0* program (Figure 1d).<sup>31</sup> Although the adjacent layers are packed in an ABCABC arrangement (Figure S2), the stacking still leads to two different types of one-dimensional (1D) opening channels with effective size of  $8.9 \times 8.0$  Å<sup>2</sup> and  $9.3 \times 7.8$  Å<sup>2</sup> along *a*- and *c*- axis, respectively (Figure 1e and 1f), in which the void space is filled with DMF molecules. PLATON<sup>32</sup> calculation suggests a solvent accessible volume of 507.1 Å<sup>3</sup> (39.6 % of unit cell) by excluding the guest solvent molecules.

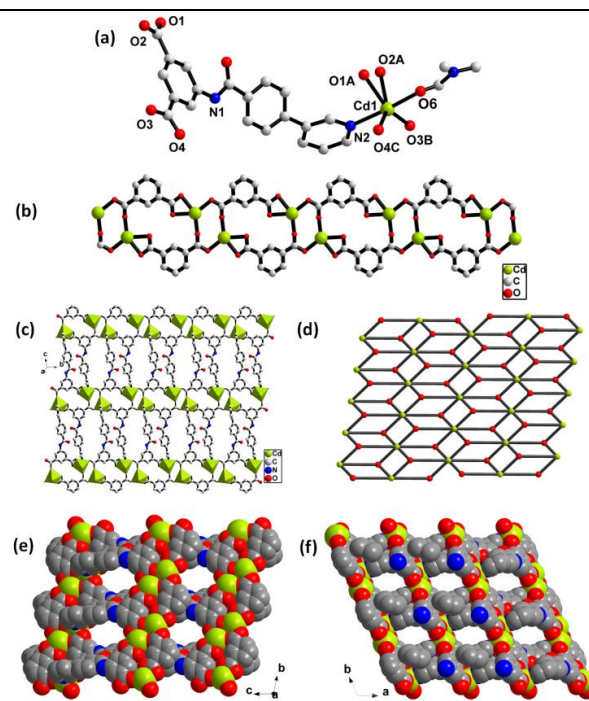


**Figure 1.** Crystal structure of Cd-PBA. (a) Coordination environment of Cd(II). (b) 1D chain connected through the carboxylate groups in Cd-PBA. (c) Polyhedral view of 2D network. (d) View of the (3,6)-connected kgd net topology with the Schläfli symbol of  $(4^3)_2(4^6.6^6.8^3)$ . A space-filling view of the porous network showing two different types of 1D channels along the crystallographic (e) *a*-axis, and (f) *c*-axis, in which the solvent molecules are omitted for clarity. All hydrogen atoms are omitted for clarity.

Field emission scanning electron microscopy (FESEM) and transmission electron microscopy (TEM) were firstly applied to observe the morphology of the as-prepared Cd-PBA samples. As presented in Figure S3, the average size of MOF particle is approximate to be 3  $\mu\text{m}$ . To confirm the phase purity of Cd-PBA, PXRD pattern for the bulk samples was measured at room temperature. Figure S4 shows that all the diffraction peaks perfectly match well with the simulated pattern results, confirming the phase purity of the obtained crystal samples. The intensity differences may be due to the preferred orientation of the crystalline samples.

Meanwhile, thermogravimetric analysis (TGA) for crystal samples was also performed under nitrogen atmosphere. As shown in Figure S5, the TG curve in the range of 100–150  $^{\circ}\text{C}$  shows a first loss of 12.52 %, corresponding to the loss of one solvent DMF molecule (calcd. 12.61 %). The second weight loss of 11.71 % ranges from 150 to 400  $^{\circ}\text{C}$  due to the loss of one coordinated DMF molecule (calcd 11.81 %). Above 500  $^{\circ}\text{C}$ , an abrupt weight loss appears, which is ascribed to the decomposition of the framework. The final residual after thermal decomposition was presumed to be CdO (found 21.1 %, calcd 20.7 %).

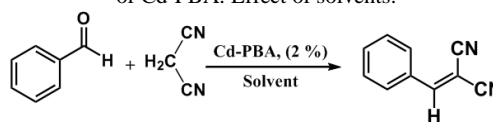
Nitrogen sorption experiments were carried out to evaluate the pore characteristics. To activate the sample, the fresh samples were immersed in  $\text{CH}_3\text{OH}$  solvent for three days, then was heated under vacuum at 120  $^{\circ}\text{C}$  for 5 h to remove all the solvent molecules, generating the dehydrated phase Cd-PBA. No obvious weight loss of the dehydrated phase was observed at the starting temperature (Figure S6), suggesting the complete removal of all the uncoordinated and coordinated solvent molecules. Moreover, PXRD pattern further confirmed that the framework remained intact and the preservation of its crystallinity (Figure S4). Based on the nitrogen adsorption/desorption isotherms in Figure S7, the porous Cd-PBA exhibited typical type-I curve with a Brunauer-Emmett-Teller surface area of 768  $\text{m}^2 \text{g}^{-1}$  and a total pore volume of 0.47  $\text{cm}^3 \text{g}^{-1}$ . The pore-size distribution calculated by Barrett-Horvath-Kawazoe (HK) method reveals the pore diameter is about 8.5  $\text{\AA}$ , which is agreement with the crystal structure analysis (Figure S8). This porous and robust framework property could provide a platform to carry out heterogeneous catalytic reaction.

**3.2. Catalytic Performances.** It is interesting to note that there exists the  $-\text{NH}$  groups of amides in the framework, suggesting that desolvated Cd-PBA might serve as an active catalyst for Lewis base promoted reactions. Therefore, the Lewis base-catalyzed Knoevenagel condensation reactions of carbonyl compounds with malononitrile in the presence of Cd-PBA as catalyst were carried out. As we know, the Knoevenagel reaction is a weakly basic condensation reaction, as an important member of the C-C bond formation reaction family, which is employed in the synthesis of fine chemicals and pharmaceutical products.<sup>33–35</sup> Because Cd-PBA is insoluble in most organic solvents, we used ethanol, cyclohexane, *n*-hexane, acetonitrile, benzene, dichloromethane, tetrahydrofuran, and DMF as solvents. As shown in Table 1, the reaction yields in ethanol and benzene solvents were more

accelerated in comparison with other organic solvents. However, due to the toxicity of benzene solvent, we used the ethanol as catalytic solvent instead in this case.

Herein, we employed a molar ratio of 1:2 to select aromatic benzaldehyde and malononitrile compounds in ethanol at room temperature for 2 h with 2 % catalyst loading, which generated the corresponding product yield of 91 % for 2 h (Table 1, entry 1). The yield is slightly less than the powerful Lewis base catalyst  $[\text{Cd}_3(\text{tipp})(\text{bpdc})_2]$  with a 93 % conversion after 1 h with 0.6 % catalyst loading.<sup>36</sup> However, the experimental condition was conducted at the temperature of 60  $^{\circ}\text{C}$ . Meanwhile, our catalyst presents a significant improvement compared to the other reported MOFs catalysts.<sup>37–41</sup> For comparison, a series of control experiments were conducted. Obviously, when the reaction was carried out in the absence of catalyst, only 6 % conversion of target products were achieved, demonstrating the excellent catalytic performance of Cd-PBA for the formation of C-C bond. Additionally, to verify the active sites, we used  $\text{Cd}(\text{NO}_3)_2 \cdot 4\text{H}_2\text{O}$  as homogeneous catalyst instead of Cd-PBA, however, a negligible conversion of 3 % was observed. By utilizing the  $\text{H}_2\text{PBA}$  ligand as catalyst, which can catalyze the reaction with a yield of 39 % under the similar condition. Furthermore, when  $\text{Cd}(\text{NO}_3)_2 \cdot 4\text{H}_2\text{O}$  was used as a catalyst,  $\text{H}_2\text{PBA}$  ligand was utilized as additive, a moderate yield of 31 % was observed. These results indicate that  $-\text{NH}$  groups of amides have influence on promoting the catalytic reaction. When the unactivated Cd-PBA samples were used instead of the activated ones, the catalytic results are inferior to that of dehydrated Cd-PBA under the similar conditions (Yield: 54 %), which indicates that the catalytic active sites might be easily blocked by the solvent molecule, and the substrates have to compete with the solvent molecules during the catalytic process.<sup>42</sup>

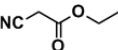
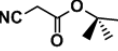
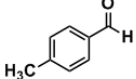
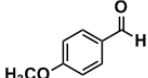
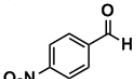
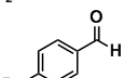
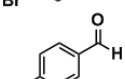
**Table 1.** Reaction of benzaldehyde with malononitrile in the presence of Cd-PBA: Effect of solvents.



| Entry | Solvent          | Time (h) | Yield <sup>[a]</sup> (%) | Isolated yield <sup>[b]</sup> (%) |
|-------|------------------|----------|--------------------------|-----------------------------------|
| 1     | Ethanol          | 2        | 91                       | 86                                |
| 2     | Cyclohexane      | 6        | 51                       | 40                                |
| 3     | <i>n</i> -Hexane | 6        | 57                       | 42                                |
| 4     | Acetonitrile     | 4        | 72                       | 65                                |
| 5     | Benzene          | 2        | 92                       | 85                                |
| 6     | Dichloromethane  | 8        | 6                        | –                                 |
| 7     | Tetrahydrofuran  | 6        | 75                       | 58                                |
| 8     | DMF              | 10       | 8                        | –                                 |

<sup>a</sup> Reaction conditions: catalyst (0.02 mmol), benzaldehyde (1 mmol), malononitrile (2 mmol), solvent (5 mL). Yield determined by <sup>1</sup>H NMR analysis using  $\text{CH}_2\text{Br}_2$  as an internal standard. <sup>b</sup> Isolated yield after column chromatography.

**Table 2.** Knoevenagel condensation reactions catalyzed by Cd-PBA<sup>a</sup>

| Entry | Substrate   | Substrate   | Yield <sup>[b]</sup> (%) | Isolated yield (%) |
|-------|---|---|--------------------------|--------------------|
| 1     |    |    | 91 <sup>[c]</sup>        | 86                 |
|       |   |   | 6 <sup>[d]</sup>         | —                  |
|       |   |   | 39 <sup>[e]</sup>        | 25                 |
|       |   |   | 31 <sup>[f]</sup>        | 21                 |
| 2     |    |    | 37 <sup>[f]</sup>        | 22                 |
|       |   |   | 5 <sup>[f]</sup>         | —                  |
| 3     |    |    | 4 <sup>[f]</sup>         | —                  |
| 4     |    |    | 42 <sup>[f]</sup>        | 34                 |
| 5     |    |    | 61 <sup>[f]</sup>        | 48                 |
|       |   |   | 15 <sup>[f]</sup>        | —                  |
| 6     |    |    | 65 <sup>[f]</sup>        | 51                 |
|       |   |   | 19 <sup>[f]</sup>        | —                  |
| 7     |    |    | >99 <sup>[f]</sup>       | 88                 |
|       |   |   | 37 <sup>[f]</sup>        | —                  |
| 8     |   |   | >99                      | 90                 |
|       |   |   | 40 <sup>[f]</sup>        | 27                 |
| 9     |  |  | >99                      | 86                 |
|       |   |   | 41 <sup>[f]</sup>        | 27                 |

<sup>a</sup> Reaction conditions: catalyst (0.02 mmol), benzaldehyde (1 mmol), malononitrile (2 mmol), ethanol (5 mL), room temperature, 2 h. <sup>b</sup> Yield was determined by <sup>1</sup>HNMR with CH<sub>2</sub>Br<sub>2</sub> as an internal standard. <sup>c</sup> The same reaction conditions without catalyst. <sup>d</sup> Catalyzed by Cd(NO<sub>3</sub>)<sub>3</sub>·4H<sub>2</sub>O. <sup>e</sup> Catalyzed by H<sub>2</sub>PBA ligands. <sup>f</sup> Catalyzed by a mixture of Cd(NO<sub>3</sub>)<sub>3</sub>·6H<sub>2</sub>O and H<sub>2</sub>PBA ligands. <sup>g</sup> Catalyzed by the as-made samples of Cd-PBA without activation.

To expand the scope of Cd-PBA catalyst for Knoevenagel condensation reaction, various substrates were treated under the similar condition. On one hand, substrates with different size and shape have apparent effect on the product yields (Table 2, entries 1-3). As evident from Table 2, substrates of increasing dimensions are also tested. As for ethyl cyanoacetate (3.4 × 7.3 Å<sup>2</sup>), the product yield was 37 % in 2 h (Table 2, entry 2). In the case of the even larger *tert*-butyl cyanoacetate (4.3 × 8.2 Å<sup>2</sup>), the reaction almost did not proceed (Table 2, entry 3). With the size of the benzaldehyde derivatives further increases, for example, 1-naphthaldehyde (5.9 × 7.2 Å<sup>2</sup>), the yield decreased obviously to 42 % under the same conditions (Table 2, entry 4). Similar size-selective behaviors can also be observed in the previously reported MOF-based heterogeneous catalysts.<sup>43,44</sup> Moreover, we performed the FT-IR experiments of Cd-PBA catalyst before and after catalytic reactions (Figure 2). By simply immersing the as-prepared Cd-PBA samples in benzaldehyde solution for

2 h, some small peaks between 2820 and 2742 cm<sup>-1</sup> appeared in the IR spectrum of the solid sample, confirming the presence of aldehyde (-CHO) in the porous framework. On the other hand, the IR spectrum of Cd-PBA after catalytic reaction displayed a small peak at 2216 cm<sup>-1</sup> resulted from the C≡N vibration characteristics, implying the presence of cyano-group in the Cd-PBA catalyst. In order to get insight into the influence of different substituents in the aromatic aldehydes, a variety of benzaldehyde derivatives with active methylene compounds were selected as substrates. The electronic groups on the aromatic aldehydes have a significant effect on the reaction outcome (entries 5-9). Aldehydes with electron-withdrawing groups provide higher yield than those with electron-donating ones. As shown in Table 2, benzaldehyde derivatives bearing electron-withdrawing groups, such as 4-nitrobenzaldehyde, 4-hydroxybenzaldehyde, and 4-bromobenzaldehyde, are fully converted to the catalytic products with the highest conversion of 100 % after 2 h (entries 7-9). Nevertheless, malononitrile reacted with electron-donating groups, such as 4-methylbenzaldehyde and 4-methoxybenzaldehyde, give relatively low product yields (entries 5-6). The tendency could be explained by the faster activation and higher electropositive charge on the carbonyl group due to nucleophilic attack, resulting in an excellent conversions in the catalytic reactions.<sup>45,46</sup> In contrast, the activation of carbonyl group is lower in the presence of electron-donating groups, leading to a lower yield in the nucleophilic reactions.

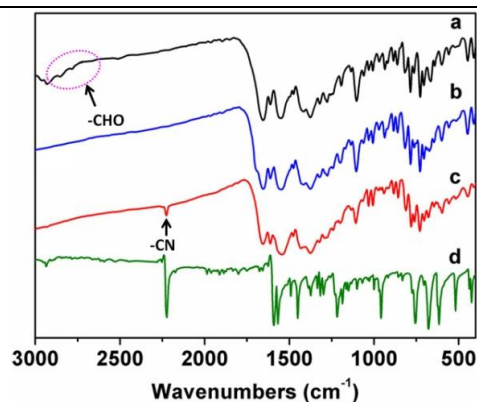


**Figure 2.** FI-IR spectra. (a) solid samples of Cd-PBA soaked in benzaldehyde solvent; (b) as-prepared Cd-PBA; (c) samples of Cd-PBA after catalytic reaction; and (d) benzalmalononitrile.

To check the heterogeneous property of Cd-PBA catalyst, we carried out a filtering experiment. The catalysts were filtered off after 1 h and the filtrate was allowed to stand under stirring (Figure 3). It was noticed that the conversion almost unchanged in the following 60 min, demonstrating the heterogeneity of the reaction.

PXRD pattern was further applied to verify the framework robustness of the recovered Cd-PBA sample. As depicted in Figure S4, similar diffraction peaks can be observed before and after the reaction, indicating the integrity of the framework structure. It is noticed that the catalyst can be simply filtrated from the reaction system and recycled for four times without obvious decrease during the reaction (Figure 4).

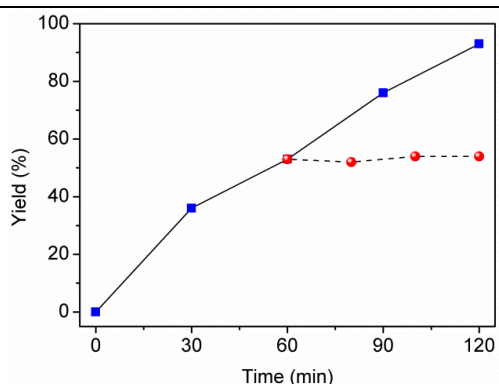


**Figure 3.** Yield of Knoevenagel condensation reaction in the presence of Cd-PBA and the filtrate of the reaction after 1h.

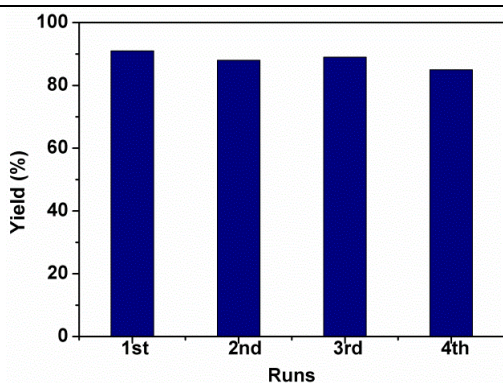


**Figure 4.** Recycling test for reaction between benzaldehyde and malononitrile in the presence of Cd-PBA.

Considering the rich open metal sites in the whole framework, the acid-catalyzed cyanosilylation of aromatic aldehydes were also carried out as the model reaction. As is well-known, cyanosilylation reaction can be applied to obtain cyanohydrins for both organic synthesis and biological processes.<sup>47</sup> Moreover, previous reports have shown that porous MOFs with coordinatively unsaturated sites could promote the catalytic efficiencies for cyanosilylation reaction, leading to the formation of C-C bond.<sup>48-50</sup> Herein, benzaldehyde (1 mmol) and trimethylsilylcyanide (TMSCN, 2 mmol) was reacted in *n*-hexane solvent with a catalyst loading of 2 % Cd-PBA at room temperature. As presented in Table 3, Cd-PBA catalyst provides a 100 % yield after 8 h, showing enhanced catalytic efficiency compared with those of the previously reported MOFs.<sup>51-53</sup> For example, Tm(BDC)<sub>1.5</sub> reported by Sun afforded a moderate conversion of 57.4 % of benzaldehyde after 5 h.<sup>54</sup> The catalyst loading of 11 mol % Mn<sub>3</sub>[(Mn<sub>4</sub>Cl)<sub>3</sub>(BTT)<sub>8</sub>]<sub>2</sub> gave a 98 % yield after 9 h.<sup>55</sup> Cu<sub>3</sub>(BTC)<sub>2</sub>, also known as HKUST-1, offered a 57 % conversion at 313 K.<sup>56</sup> However, our catalyst presents slightly less catalytic efficiency compared with Nd(btc) catalyst, which showed 99 % yield with a catalyst loading of 9.0 % after 2 h.<sup>57</sup> Given the high catalytic activity of Cd-PBA, we further evaluate the scope of substrates. As for 1-naphthaldehyde, the product yield of 58 % was obtained after 8 h (Table 3, entry 2). In the case of larger 4-phenylbenzaldehyde, the yield reduced to 18 % under the same conditions (Table 3, entry 3). Moreover, acetophenone was also used as substrate; however,

a negligible conversion of 12 % was achieved under the similar conditions due to its innate reduced reactivity (Table 3, entry 9). Similarly, aldehydes with electron-withdrawing groups are more reactive than those with electron-donating ones. As shown in Table 3, benzaldehyde derivatives bearing electron-donating groups (-CH<sub>3</sub>, -OCH<sub>3</sub>) give relatively low product yields (entries 4-5). Nevertheless, malononitrile reacted with electron-withdrawing benzaldehyde derivatives (-NO<sub>2</sub>, -OH, and -Br) are completely converted to the corresponding products with the highest yield after 2 h (entries 6-8). For comparison, we also used the unactivated MOF as the heterogeneous catalyst. However, a moderate yield of 35% was detected under the similar catalytic conditions. The relative catalytic activity ratio of unactivated MOF vs activated MOF is 0.35, suggesting that the substrates have to compete with the solvent molecules in the framework and have less chances to access the metal centers.

**Table 3.** Cyanosilylation of aromatic aldehydes in the presence of Cd-PBA<sup>a</sup>

| Entry | Substrate | Product | Yield <sup>[b]</sup> (%)                     | Isolated yield <sup>[c]</sup> (%) |
|-------|-----------|---------|--|-----------------------------------|
| 1     |           |         | >99<br>35 <sup>[d]</sup><br>7 <sup>[e]</sup> | 89<br>—<br>—                      |
| 2     |           |         | 58<br>2 <sup>[e]</sup>                       | 40<br>—                           |
| 3     |           |         | 18<br>0 <sup>[e]</sup>                       | —<br>—                            |
| 4     |           |         | 69<br>0 <sup>[e]</sup>                       | 55<br>—                           |
| 5     |           |         | 73<br>0 <sup>[e]</sup>                       | 58<br>—                           |
| 6     |           |         | >99<br>12 <sup>[e]</sup>                     | 91<br>—                           |
| 7     |           |         | >99<br>9 <sup>[e]</sup>                      | 85<br>—                           |
| 8     |           |         | >99<br>10 <sup>[e]</sup>                     | 88<br>—                           |
| 9     |           |         | 12<br>0 <sup>[e]</sup>                       | —<br>—                            |

<sup>a</sup> catalyst (2 %), benzaldehyde (1 mmol), TMSCN (2 mmol), 5mL of *n*-hexane, room temperature, 8 h. <sup>b</sup> Yields determined by <sup>1</sup>H NMR spectroscopy by using CH<sub>2</sub>Br<sub>2</sub> as an internal standard. <sup>c</sup> Isolated yield after column chromatography. <sup>d</sup> Catalyzed by the unactivated Cd-PBA. <sup>e</sup> Catalyzed by a mixture of Cd(NO<sub>3</sub>)<sub>2</sub>·6H<sub>2</sub>O and H<sub>2</sub>PBA ligands.

Moreover, we also carried out the control experiments for both catalytic cyanosilylation and Knoevenagel condensation reactions by using H<sub>2</sub>PBA and Cd(NO<sub>3</sub>)<sub>2</sub>·4H<sub>2</sub>O as catalysts instead of Cd-PBA, respectively, including those substrates with different sizes and electronic properties. In the case of Knoevenagel condensation reactions, moderate yield of the corresponding products could be obtained (Table 2), such as 31 % for benzaldehyde, 15% for 4-methylbenzaldehyde, 19 % for 4-methoxybenzaldehyde, 41% for 4-hydroxybenzaldehyde, 40% for 4-bromobenzaldehyde, and 37% for 4-nitrobenzaldehyde. These results show that the catalytic centers mainly result from the -NH groups of amides. However, as for the cyanosilylation reactions, all the result show the inferior product yields and the negligible yield below 10 % can be detected for all the substrates (Table 3). These observations reveal the catalytic sites are ascribed to the coordinatively unsaturated metal centers. The Cd<sup>2+</sup> ion in Cd(NO<sub>3</sub>)<sub>2</sub>·4H<sub>2</sub>O is eight-coordinated environment with four H<sub>2</sub>O molecules at the equatorial positions and four oxygen atoms from two nitrate ions at the apical positions.<sup>58</sup> As a result, the Cd center of Cd(NO<sub>3</sub>)<sub>2</sub>·4H<sub>2</sub>O is blocked by the coordinated water molecules, making more difficult to access to the substrates.

#### 4. CONCLUSION

In summary, we presented a stable 2D Cd(II)-based metal-organic framework with kgd net topology. Such a MOF features bifunctional property with the combination of Lewis basic sites and open metal sites as efficient heterogeneous catalysis for the C-C bond formation, such as Knoevenagel condensation reaction and cyanosilylation of aromatic aldehydes. Both of the basic-catalysed and acidic-catalysed reactions, Cd-PBA exhibits higher catalytic activities to electron-withdrawing benzaldehyde derivatives compared with those with electron-donating groups during the catalytic process. More importantly, this MOF can be reused for several times without loss of obvious catalytic efficiency. The excellent catalytic activity and good stability prove Cd-PBA to be an efficient catalyst for the formation of C-C bond.

#### ASSOCIATED CONTENT

##### Supporting Information

Crystallographic data, SEM and TEM images, PXRD patterns, TGA curves, N<sub>2</sub> adsorption/desorption isotherms, and pore-size distribution. This material is available free of charge via the Internet at <http://pubs.acs.org>.

##### Corresponding Author

\*E-mail: [linxm@scnu.edu.cn](mailto:linxm@scnu.edu.cn).

\*E-mail: [caiy@scnu.edu.cn](mailto:caiy@scnu.edu.cn).

##### Notes

The authors declare no competing financial interest.

#### ACKNOWLEDGMENT

We gratefully acknowledge the financial support from the National Natural Science Foundation of China (Grant Nos. 21401059, 21671071 and 21471061), Science and Technology Planning Project of Guangdong Province (2017A010104015, 2017B090917002 and 2015B010135009), Open Project of State Key Laboratory of Structural Chemistry (20150013), Innovation

Team Project of Guangdong Ordinary University (No. 2015KCXTD005), and the Great Scientific Research Project of Guangdong Ordinary University (No. 2016KZDXM023).

#### REFERENCES

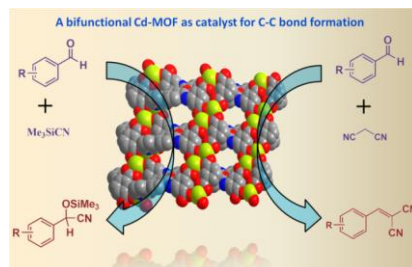
- (1) Wang, C.; Li, L.; Bell, J. G.; Lv, X.; Tang, S.; Zhao, X.; Thomas, K. M. *Chem. Mater.* **2015**, *27*, 1502–1516.
- (2) Pan, M.; Zhu, Y.-X.; Wu, K.; Chen, L.; Hou, Y.-J.; Yin, S.-Y.; Wang, H.-P.; Fan, Y.-N.; Su, C.-Y. *Angew. Chem. Int. Ed.* **2017**, *56*, 14582–14586.
- (3) Huang, X. F.; Ma, J. X.; Liu, W. S. *Inorg. Chem.* **2014**, *53*, 5922–5930.
- (4) Wu, P.; He, C.; Wang, J.; Peng, X.; Li, X.; An, Y.; Duan, C. J. *Am. Chem. Soc.* **2012**, *134*, 14991–14999.
- (5) Jiang, J. J.; Yang, R.; Xiong, Y.; Li, L.; Pan, M.; Su, C. Y. *Sci. China Chem.* **2011**, *54*, 1436–1440.
- (6) Fu, L.; Liu, Y.; Pan, M.; Kuang, X.-J.; Yan, C.; Li, K.; Wei, S.-C.; Su, C.-Y. *J. Mater. Chem. A* **2013**, *1*, 8575–8580.
- (7) Zhang, J.; Biradar, A. V.; Pramanik, S.; Emge, T. J.; Asefa, T.; Li, J. *Chem. Commun.* **2012**, *48*, 6541–6543.
- (8) Cao, L.; Lin, Z.; Peng, F.; Wang, W.; Huang, R.; Wang, C.; Yan, J.; Liang, J.; Zhang, Z.; Zhang, T.; Long, L.; Sun, J.; Lin, W. *Angew. Chem. Int. Ed.* **2016**, *55*, 4962–4966.
- (9) Lin, Z.; Thacker, N. C.; Sawano, T.; Drake, T.; Ji, P.; Lan, G.; Cao, L.; Liu, S.; Wang, C.; Lin, W. *Chem. Sci.* **2018**, *9*, 143–151.
- (10) Zhu, Y.; Zhu, M.; Xia, L.; Wu, Y.; Hua, H.; Xie, J. *Sci. Rep.* **2016**, *6*, 29728–29739.
- (11) Chen, J.; Shen, K.; Li, Y. *ChemSusChem* **2017**, *10*, 3165–3187.
- (12) Chen, L.; Huang, W.; Wang, X.; Chen, Z.; Yang, X.; Luque, R.; Li, Y. *Chem. Commun.* **2017**, *53*, 1184–1187.
- (13) Liu, H.; Chang, L.; Bai, C.; Chen, L.; Luque, R.; Li, Y. *Angew. Chem. Int. Ed.* **2016**, *55*, 5019–5023.
- (14) Chen, L.; Huang, B.; Qiu, X.; Wang, X.; Luque, R.; Li, Y. *Chem. Sci.* **2016**, *7*, 228–233.
- (15) Yoon, M.; Srirambalaji, R.; Kim, K. *Chem. Rev.* **2011**, *112*, 1196–1231.
- (16) Tao, L.; Lin, C. Y.; Dou, S.; Feng, S.; Chen, D. W.; Liu, D. D.; Huo, J.; Xia, Z. H.; Wang, S. Y. *Nano Energy* **2017**, *41*, 417–425.
- (17) Ren, H. Y.; Yao, R. X.; Zhang, X. M. *Inorg. Chem.* **2015**, *54*, 6312–6318.
- (18) Kong, G. Q.; Ou, S.; Zou, C.; Wu, C. D. *J. Am. Chem. Soc.* **2016**, *138*, 8352–8355.
- (19) Chen, D. P.; Luo, R.; Li, M. Y.; Wen, M. Q.; Li, Y.; Chen, C.; Zhang, N. *Chem. Commun.* **2017**, *53*, 10930–10933.
- (20) Xia, M.; Zhuo, C.; Ma, X.; Zhang, X.; Sun, H.; Zhai, Q.; Zhang, Y. *Chem. Commun.* **2017**, *53*, 11302–11305.
- (21) Gu, J. M.; Kim, W. S.; Huh, S. *Dalton Trans.* **2011**, *40*, 10826–10829.
- (22) Lin, X. M.; Li, T. T.; Chen, L. F.; Zhang, L.; Su, C. Y. *Dalton Trans.* **2012**, *41*, 10422–10429.
- (23) Lin, X. M.; Li, T. T.; Wang, Y. W.; Zhang, L.; Su, C. Y. *Chem. Asian J.* **2012**, *7*, 2796–2804.
- (24) Lin, X. M.; Niu, J. L.; Wen, P. X.; Lu, Y. N.; Hu, L.; Zhang, D. L.; Cai, Y. P. *RSC Adv.* **2016**, *6*, 63425–63432.
- (25) Lin, X. M.; Niu, J. L.; Wen, P. X.; Pang, Y.; Hu, L.; Cai, Y. P. *Cryst. Growth Des.* **2016**, *16*, 4705–4710.
- (26) Ding, Y. J.; Zhang, C. P.; Wang, Y. Q.; Zhu, X. M.; Lin, X. M.; Zhang, D. L.; Duan, X. J.; Cai, Y. P. *CrystEngComm* **2015**, *17*, 6693–6698.
- (27) Niu, J. L.; Hao, G. X.; Lin, J.; He, X. B.; Sathishkumar, P.; Lin, X. M.; Cai, Y. P. *Inorg. Chem.* **2017**, *56*, 9966–9972.
- (28) Peng, H. J.; Hao, G. X.; Chu, Z. H.; Cui, Y. L.; Lin, X. M.; Cai, Y. P. *Inorg. Chem.* **2017**, *56*, 10007–10012.
- (29) Peng, H. J.; Hao, G. X.; Chu, Z. H.; Lin, J.; Lin, X. M.; Cai, Y. P. *Cryst. Growth Des.* **2017**, *17*, 5881–5886.
- (30) Sheldrick, G. M. *Acta Cryst.* **2015**, *C71*, 3–8.
- (31) Blatov, V. A.; Shevchenko, A. P.; Proserpio, D. M. *Cryst. Growth Des.* **2014**, *14*, 3576–3586.

- 1 (32) Spek, A. L. *Acta Crystallogr. Sect. C: Struct. Chem.* **2015**, *71*,  
2 9–18.
- 3 (33) Gascon, J.; Aktay, U.; Hernandez-Alonso, M. D.; van Klink, G.  
4 P. M.; Kapteijn, F. *J. Catal.* **2009**, *261*, 75–87.
- 5 (34) Hasegawa, S.; Horike, S.; Matsuda, R.; Furukawa, S.;  
6 Mochizuki, K.; Kinoshita, Y.; Kitagawa, S. *J. Am. Chem. Soc.* **2007**,  
7 *129*, 2607–2614.
- 8 (35) Fang, Q. R.; Yuan, D. Q.; Sculley, J.; Li, J. R.; Han, Z. B.; Zhou,  
9 H. C. *Inorg. Chem.* **2010**, *49*, 11637–11642.
- 10 (36) Jiang, W.; Yang, J.; Liu, Y. Y.; Song, S. Y.; Ma, J. F. *Inorg.*  
11 *Chem.* **2017**, *56*, 3036–3043.
- 12 (37) Ugale, B.; Sandeep, S. D.; Nagaraja, C. M. *Inorg. Chem. Front.*  
13 **2017**, *4*, 348–359.
- 14 (38) Wang, X. S.; Liang, J.; Li, L.; Lin, Z. J.; Bag, P. P.; Gao, S. Y.;  
15 Huang, Y. B.; Cao, R. *Inorg. Chem.* **2016**, *55*, 2641–2649.
- 16 (39) Fang, Q. R.; Yuan, D. Q.; Sculley, J.; Li, J. R.; Han, Z. B.; Zhou,  
17 H. C. *Inorg. Chem.* **2010**, *49*, 11637–11642.
- 18 (40) Li, X. L.; Zhang, B. Y.; Fang, Y. H.; Sun, W. J.; Qi, Z. Y.; Pei,  
19 Y. C.; Qi, S. Y.; Yuan, P. Y.; Luan, X. C.; Goh, T. W.; Huang, W. Y.  
20 *Chem. Eur. J.* **2017**, *23*, 4266–4270.
- 21 (41) Huang, J. P.; Li, C. M.; Tao, L. L.; Zhu, H. L.; Hu, G. *J. Mol.*  
22 *Struct.* **2017**, *1146*, 853–860.
- 23 (42) Shi, L. X.; Wu, C. D. *Chem. Commun.* **2011**, *47*, 2928–2930.
- 24 (43) Fan, W. D.; Wang, Y. T.; Xiao, Z. Y.; Zhang, L. L.; Gong, Y.  
25 Q.; Dai, F. N.; Wang, R. M.; Sun, D. F. *Inorg.*  
26 *Chem.* **2017**, *56*, 13634–13637.
- 27 (44) Luo, Q. X.; Song, X. D.; Park, S. E.; Hao, C.; Li, Y. Q.; *Appl.*  
28 *Catal. A-Gen.* **2014**, *478*, 81–90.
- 29 (45) Ugale, B.; Dhankhar, S. S.; Nagaraja, C. M. *Inorg. Chem. Front.*  
30 **2017**, *4*, 348–359.
- 31 (46) Ugale, B.; Nagaraja, C. M. *RSC Adv.* **2016**, *6*, 28854–28864.
- 32 (47) Hatano, M.; Yamakawa, K.; Kawai, T.; Horibe, T.; Ishihara, K.  
33 *Angew. Chem., Int. Ed.* **2016**, *55*, 4021–4025.
- 34 (48) Karmakar, A.; Rúbio G. M. D. M.; Paul, A.; Silva Guedes da,  
35 M. F. C.; Mahmudov, K. T.; Guseinov, F. I.; Carabineiro, S. A.  
36 C.; Pombeiro, A. J. L. *Dalton Trans.* **2017**, *46*, 8649–8657.
- 37 (49) D’Vries, R. F.; Iglesias, M.; Snejko, N.; Gutiérrez-Puebla, E.;  
38 Monge, M. A. *Inorg. Chem.* **2012**, *51*, 11349–11355.
- 39 (50) Liu, L.; Han, Z. B.; Wang, S. M.; Yuan, D. Q.; Ng, S. W. *Inorg.*  
40 *Chem.* **2015**, *54*, 3719–3721.
- 41 (51) Fujita, M.; Kwon, Y. J.; Washizu, S.; Ogura, K. *J. Am. Chem.*  
42 *Soc.* **1994**, *116*, 1151–1152.
- 43 (52) Liu, X.; Lin, H.; Xiao, Z.; Fan, W.; Huang, A.; Wang, R.;  
44 Zhang, L.; Sun, D. *Dalton Trans.* **2016**, *45*, 3743–3749.
- 45 (53) Horike, S.; Dincă, M.; Tamaki, K.; Long, J. R. *J. Am. Chem.*  
46 *Soc.* **2008**, *130*, 5854–5855.
- 47 (54) He, H. Y.; Ma, H. Q.; Sun, D.; Zhang, L. L.; Wang, R. M.;  
48 Sun, D. F. *Cryst. Growth Des.* **2013**, *13*, 3154–3161.
- 49 (55) Horike, S.; Dincă, M.; Tamaki, K.; Long, J. R. *J. Am. Chem.*  
50 *Soc.* **2008**, *130*, 5854–5855.
- 51 (56) Schlichte, K.; Kratzke, T.; Kaskel, S. *Micropor. Mesopor. Mat.*  
52 **2004**, *73*, 81–88.
- 53 (57) Gustafsson, M.; Bartoszewicz, A.; Martin-Matute, B.; Sun, J. L.;  
54 Grins, J. J.; Zhao, T.; Li, Z. Y.; Zhu, G. S.; Zou, X. D. *Chem. Mater.*  
55 **2010**, *22*, 3316–3322.
- 56 (58) Ohmori, O.; Fujita, M. *Chem. Commun.* **2004**, 1586–1587.

For Table of Contents Use Only

## A Bifunctional 2D Cd(II)-Based Metal-Organic Framework as Efficient Heterogeneous Catalyst for the Formation of C-C Bond

Lei Hu,<sup>†</sup> Gui-Xia Hao,<sup>‡</sup> Hai-Dong Luo,<sup>†</sup> Chun-Xian Ke,<sup>†</sup> Guang Shi,<sup>†</sup> Jia Lin,<sup>†</sup> Xiao-Ming Lin,<sup>\*,†,§</sup>  
Umair Yaqub Qazi,<sup>||</sup> and Yue-Peng Cai<sup>\*,†</sup>



A 2D porous Cd-based metal-organic framework (Cd-PBA) with kgd topology is presented. This multi-functional material shows open metal sites and Lewis basic sites for heterogeneous catalysis, which could promote the cyanosilylation reaction and Knoevenagel condensation reaction. The high catalytic activity and stability made Cd-PBA a promising catalyst toward C-C bond formation.